

Kinetics and Thermodynamics of Hydrogen Atom Exchange Reactions in Sterically Hindered Hydroxylamine–Nitroxyl Radical Systems

A. D. Malievskii, S. V. Koroteev, and A. B. Shapiro

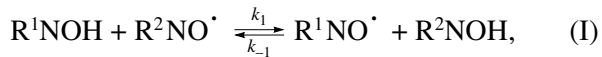
Emanuel Institute of Biochemical Physics, Russian Academy of Sciences, Moscow, 119991 Russia

Received February 10, 2004

Abstract—Rate constants and activation energies were determined for the forward and reverse hydrogen exchange reactions in systems involving a sterically hindered hydroxylamine and a nitroxyl radical of dihydroquinoline, tetrahydroquinoline, diphenylamine, imidazoline, pyrrolidine, or piperidine. The equilibrium constants and heats of these reactions were determined, and the dissociation energies of the NO–H bonds in the hydroxylamines were estimated.

The high reducing capacity of sterically hindered hydroxylamines (HAs), such as hydrogenated quinoline, diphenylamine, imidazoline, pyrrolidine, and piperidine, has recently attracted great attention because of the applicability of these HAs in a variety of chemical and biological systems [1–9], including systems in which the stable radical resulting from the reaction provides information concerning the properties of the medium. For instance, piperidine and imidazoline HAs are used to determine the rate of superoxide radical generation in microsomal membranes [1]. The hydrogen atom transfer reaction between a nitroxyl radical (NR) and a water-soluble HA of the pyrrolidine series was reported to be a tool for determining the state and accessibility of spin-labeled lipids [7]. Hydroxylamines, both in the original state and as nitroxylamines resulting from their oxidation with oxygen, superoxide radicals, or enzyme systems, are viewed as a new group of bioantioxidants capable of inhibiting free-radical processes [5, 6]. Hydroxylamines of the hydrogenated quinoline and diphenylamine series are involved in the decomposition of peroxides [4, 10].

The N–OH bond dissociation energy is one of the characteristics that should be taken into account when choosing an HA for experiments. HA–NR systems, in which hydrogen atom exchange occurs via the reaction



are promising for the study of the reactivity of HRs and HAs and can provide experimental data that are necessary for the calculation of the NO–H bond dissociation energy in HAs.

There are few kinetic and thermodynamic studies on hydrogen atom exchange in HA–NR systems [11–13]. Recently, based on experimental rate constant data for reactions between various nitroxyl radicals and hydra-

zobenzene [14], the NO–H bond dissociation energy was calculated using the parabolic model of the transition state [15–17].

In this work, the stopped-flow method with a spectrophotometric detection technique was used to study the kinetics of hydrogen atom exchange between sterically hindered HAs and NRs in order to determine the kinetic and thermodynamic parameters of this reaction and estimate the NO–H bond dissociation energies in the HAs.

EXPERIMENTAL

The HAs and the NRs of hydrogenated quinoline [18, 19], diphenylamine [20], imidazoline [12], pyrrolidine, and piperidine [21] examined in this work are presented in Fig. 1. The hydrogen atom exchange reaction was studied for HAs **1–3** and NRs **4–9** and **21**. The initial concentration of HA was $(1–4) \times 10^{-4}$ mol/l, and that of stable radicals was $(1–10) \times 10^{-4}$ mol/l.

Hydroxylamines **1–3** were obtained immediately before the experiments by reacting radicals **10–12** with slightly deficient hydrazobenzene, taking into account the stoichiometry of the reaction. Absolute hexane deoxygenated with argon was used as an inert solvent [22].

The kinetics of NR accumulation was monitored as the evolution of the absorbance of the solution at a certain wavelength: 354 nm for NR **10**, 465 nm for NR **11**, and 376 nm for NR **12**. The solution temperature was maintained in the range 10–50°C ($\pm 0.1^\circ\text{C}$). The Origin 6 program was used in the calculation of the kinetic and thermodynamic parameters of reaction (I). The error in the rate constants (k_1 and k_{-1}) of reaction (I) did not exceed 5%, and the error in the heat of reaction (ΔH) was between 5 and 15%. The NRs were purified by standard procedures.

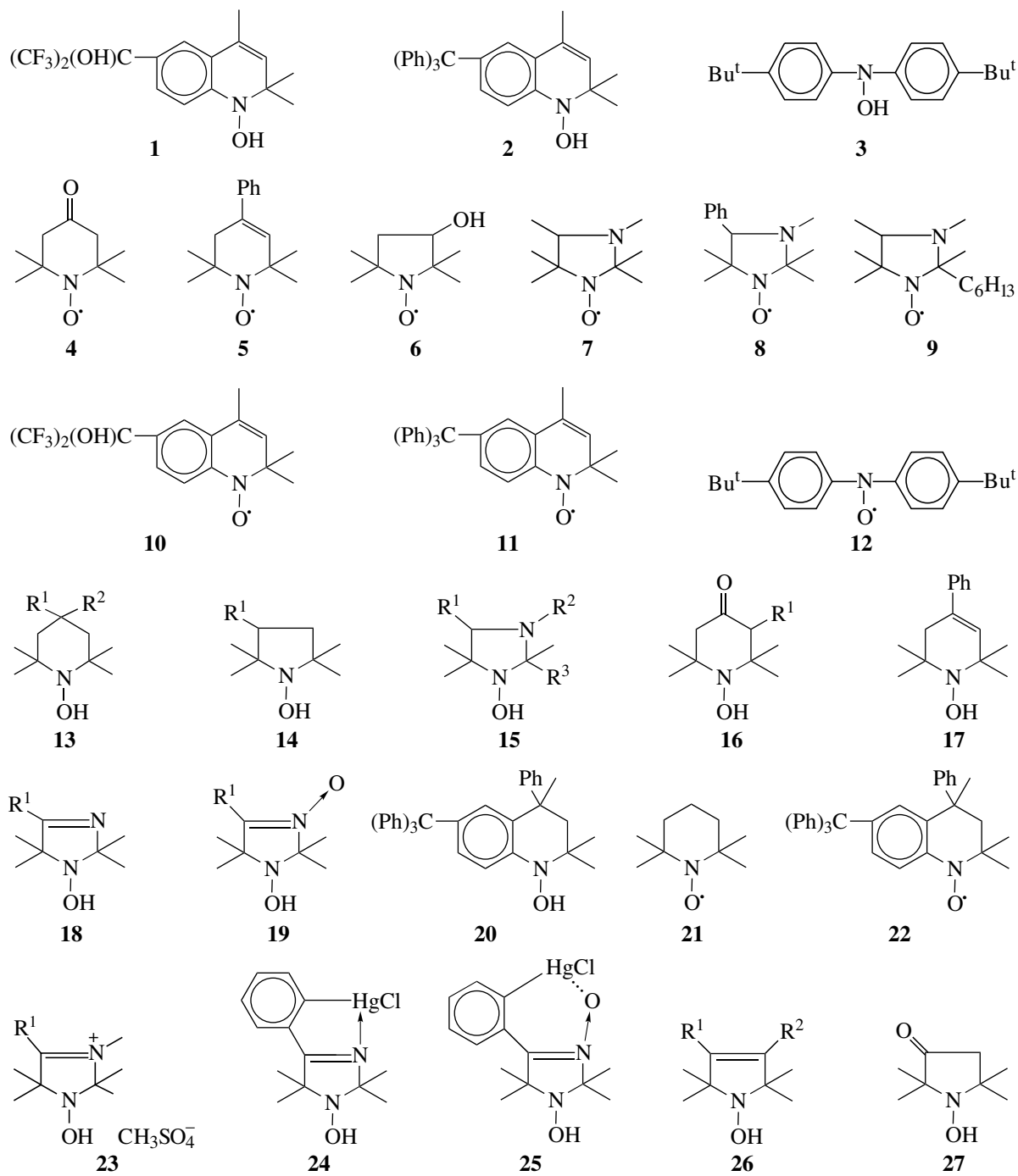


Fig. 1. The sterically hindered hydroxylamines and nitroxyl radicals considered in this study.

RESULTS AND DISCUSSION

The hydrogen atom exchange in the HA–NR systems is reversible [3, 12, 13, 23], with few exceptions [7]. The reaction between a sterically hindered HA and an NR obeys the reversible second-order rate law and is first-order with respect to either component. All of the systems under study are equilibrated 50–200 ms after the initiation of the reaction (Fig. 2).

The kinetic and thermodynamic parameters of hydrogen atom transfer in several sterically hindered HA-NR systems are listed in Table 1. As can be seen from the data in Table 1, the activation energies of the forward and reverse exchange reactions in the HA-NR systems are low, indicating a high reactivity of the species involved in hydrogen exchange. The steric factors of the forward and reverse reactions were determined.

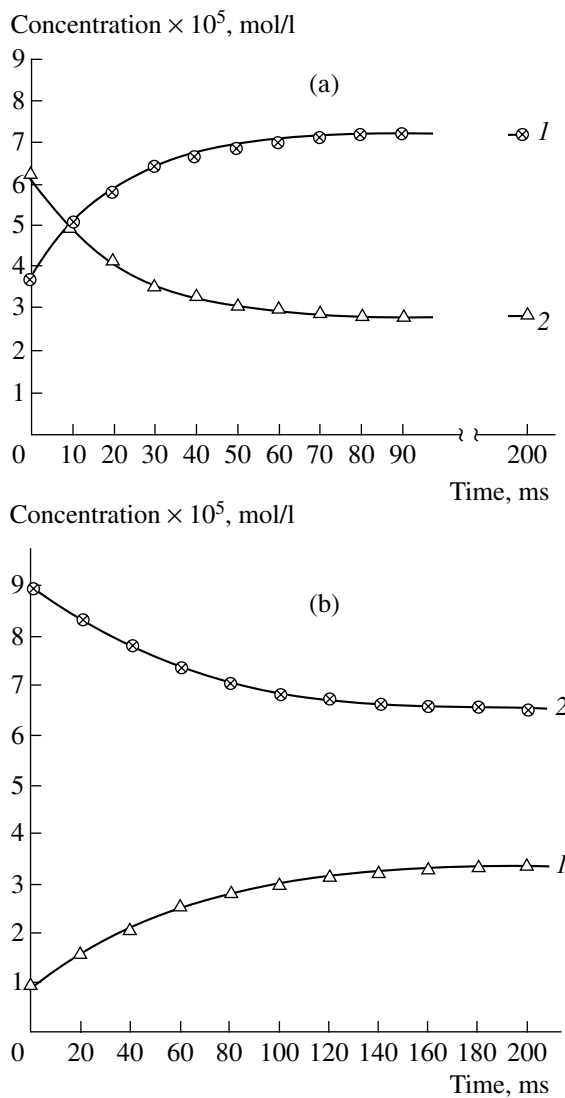


Fig. 2. (1) NR accumulation and (2) HA consumption curves for the hydrogen atom exchange reaction in the (a) NR 9–HA 2 and (b) NR 9–HA 1 systems in hexane at 25°C. (a) (1) NR 11 accumulation and (2) HA 2 consumption; $[NR 9]_0 = 1.5 \times 10^{-3}$ mol/l; $[HA 2]_0 = 6.2 \times 10^{-5}$ mol/l. (b) (1) NR 10 accumulation and (2) HA 1 consumption; $[NR 9]_0 = 3.75 \times 10^{-4}$ mol/l; $[HA 1]_0 = 9.0 \times 10^{-5}$ mol/l.

Their values ($\rho = 10^{-6}$ to 10^{-4}) are small owing to the screening of the reaction centers from the reacting species. At 25°C, the highest rates of hydrogen atom transfer were measured for the reverse reactions in the systems HA 3–HP 9, 6, and 8 ($k_{-1} = 8.0 \times 10^5$, 5.1×10^5 , and 3.5×10^5 1 mol⁻¹ s⁻¹, respectively). The lowest rates were measured for the forward reactions in the systems HA 20–NR 9, HA 1–NR 9, and HA 3–NR 9 ($k_1 = 2.5 \times 10^3$, 2.7×10^3 , and 4.0×10^3 1 mol⁻¹ s⁻¹, respectively). At 25°C, the rate constants of the forward and reverse reactions in the HA 1–NR 5 system are comparable ($k_1 = 4.3 \times 10^4$ versus $k_{-1} = 3.0 \times 10^4$ 1 mol⁻¹ s⁻¹; $K_{eq} =$

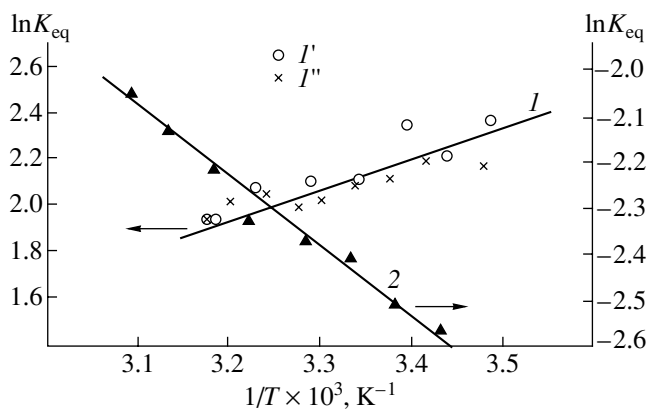


Fig. 3. Arrhenius plots of K_{eq} for the hydrogen atom exchange reaction in the (1) HA 1–NR 4 and (2) HA 1–NR 8 systems in hexane: (1) $[NR 4]_0 = (I') 2 \times 10^{-4}$ and $(I'') 4 \times 10^{-4}$ mol/l and $[HA 1]_0 = 2 \times 10^{-4}$ mol/l; (2) $[HA 1]_0 = 9.0 \times 10^{-5}$ mol/l and $[NR 8]_0 = 1 \times 10^{-3}$ mol/l.

1.43). The largest equilibrium constants ($K_{eq} = 11.10$ and 8.86) were obtained for the HA 2–NR 21 and HA 1–NR 22 systems; the smallest equilibrium constants, for the HA 3–NR 9 and HA 1–NR 9 systems [23].

The replacement of the hydrogen atom in the NO–H group of **1** and **2** with a deuterium atom (NO–D) decreases the exchange rate in the reactions between these HAs and NR 5, 7, and 8 by a factor of ~ 1.7 [23]. The isotope effect is so weak because the dissociation of the original bond and the formation of the new bond take place synchronously. The transition state is probably nearly symmetric and nearly linear.

The equilibrium constants of hydrogen atom exchange in the HA–NR systems are given in Table 1. The heats (ΔH) of the equilibrium reaction (I) for several HA–NR systems were derived from $\log K_{eq} - 1/T$ plots. In Fig. 3, we present the Arrhenius plots of K_{eq} for the HA 1–NR 4 and HA 1–NR 8 systems. In this case, ΔH is the difference between the NO–H bond strengths in the original and resulting HAs. Knowing the strength of the NO–H bond in one of the HAs and ΔH for the exchange reaction, one can estimate the dissociation energy of the NO–H bond in the other HA using the relationship

$$\Delta H = D'_{NO-H} - D''_{NO-H}, \quad (1)$$

where D''_{NO-H} and D'_{NO-H} are the dissociation energies of the NO–H bonds in the resulting and original HAs, respectively.

Hydroxylamines **1**, **2**, and **3** react with NR 4 to form NR 10, 11, and 12 and HA 16a. The NO–H bond dissociation energy in **16a** is known to be 71.9 [13] or 71.8 kcal/mol [24]. The D_{NO-H} values for HA **1**, **2**, and **3** were determined using Eq. (1) to be 69.6, 65.0, and 68.2 kcal/mol, respectively. Next, the D_{NO-H} values for

Table 1. Forward and reverse rate constants and equilibrium constants for the hydrogen atom exchange reaction in sterically hindered hydroxylamine–nitroxyl radical systems

HA	NR	$k_1, 1 \text{ mol}^{-1} \text{ s}^{-1}$	$k_{-1}, 1 \text{ mol}^{-1} \text{ s}^{-1}$	K_{eq}
1	4	$1.30 \times 10^5(\exp -420/RT)$	$5.10 \times 10^5(\exp -2520/RT)$	$0.2(\exp 2260/RT)$
		6.43×10^4	0.74×10^4	8.87
1	5	4.30×10^4	3.00×10^4	1.43
		$1.86 \times 10^5(\exp -3300/RT)$	$2.50 \times 10^5(\exp -260/RT)$	$7.4(\exp -3030/RT)$
1	6	7.33×10^3	1.62×10^5	4.6×10^{-2}
		–	–	$6.1(\exp -3080/RT)$
1	7	0.50×10^4	1.40×10^5	3.5×10^{-2}
		$1.94 \times 10^6(\exp -3160/RT)$	$2.10 \times 10^5(\exp -330/RT)$	$9.3(\exp -2830/RT)$
1	8	9.67×10^3	1.20×10^5	0.08
		$6.25 \times 10^7(\exp -6130/RT)$	$3.10 \times 10^6(\exp -1350/RT)$	$20.5(\exp -4780/RT)$
1		2.13×10^3	3.20×10^5	7×10^{-3}
	21	7.60×10^4	2.90×10^4	2.62
1	22	6.60×10^4	0.75×10^4	8.86
2	4	–	–	$3.5 \times 10^{-4}(\exp 6880/RT)$
		–	–	36
2	9	0.80×10^4	1.00×10^5	0.08
2	21	1.50×10^5	1.35×10^4	11.1
3	4	–	–	$8 \times 10^{-3}(\exp 3660/RT)$
		1.65×10^5	3.40×10^4	4.85
3	6	$5.60 \times 10^5(\exp -2200/RT)$	$6.90 \times 10^5(\exp -180/RT)$	$0.8(\exp -2020/RT)$
		1.40×10^4	5.10×10^5	2.7×10^{-2}
3	8	$5.20 \times 10^5(\exp -2180/RT)$	$6.80 \times 10^5(\exp -400/RT)$	$0.8(\exp -1780/RT)$
		1.34×10^4	3.50×10^5	0.04
3	9	0.40×10^4	0.80×10^6	5×10^{-3}
20	9	0.25×10^4	1.20×10^5	2.1×10^{-2}
20	6	0.89×10^4	5.50×10^4	0.16
20	8	0.78×10^4	5.20×10^4	0.15
20	21	5.90×10^4	1.55×10^4	3.81

Note: All constants are determined for $T = 25^\circ\text{C}$.

HA **1** and **3** were used to find $D_{\text{NO-H}}$ for the five-membered HAs **14a**, **15a**, **15b**, and **15c** using the same equation (1). For this purpose, we determined ΔH for the reactions of HAs **1** and **3** with NR **6**, of HAs **1** and **3** with NR **8**, and of HA **1** with NRs **7** and **9**. In the first case, NRs **10** and **12** and HA **14a** are formed. The $D_{\text{NO-H}}$ values

for **14a** derived from data for two reactions are close, their average being $D_{\text{NO-H}}(\text{av.}) = 66.4(\pm 0.2)$ kcal/mol. In the second case, NRs **10** and **12** and HA **15b** are formed. The $D_{\text{NO-H}}$ values for HA **15b** derived from two reactions are also close, with $D_{\text{NO-H}}(\text{av.}) = 66.7 (\pm 0.2)$ kcal/mol. Finally, the reaction of HA **1** with NR **9** yields NR **10**

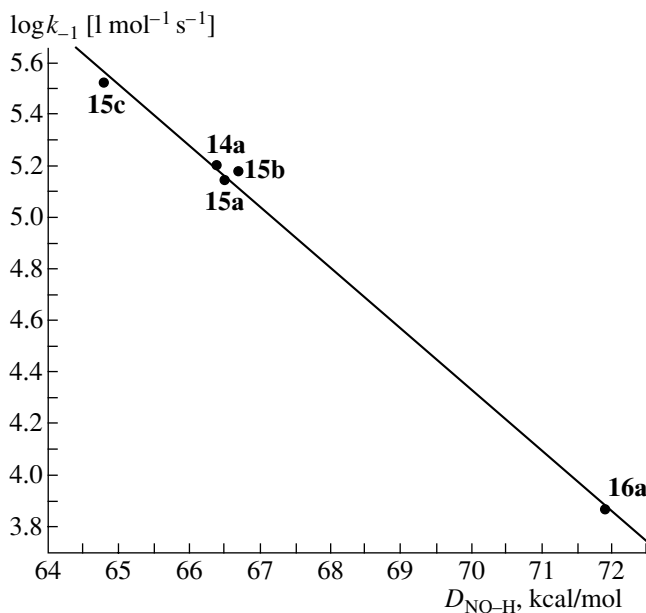


Fig. 4. $\log k_{-1}$ for the hydrogen atom exchange reaction in the systems HA **14a**–, **15a**–, **15b**–, **15c**–, and **16a**–NR **10** versus $D_{\text{NO-H}}$ in the HAs (hexane, 25°C).

and HA **15c**. For the latter, $D_{\text{NO-H}} = 64.8$ kcal/mol. The reaction between HA **1** and NR **7** produces NR **10** and HA **15a** ($D_{\text{NO-H}} = 66.5$ kcal/mol).

The dissociation energies of the NO–H bonds in HAs **14a**, **15a**, and **15b** calculated using the parabolic model of the transition state [16, 17] exceed the estimates obtained in this work by ~2.5 kcal/mol.

To estimate $D_{\text{NO-H}}$ for HAs **13a**, **17**, and **20**, we used the $\log k_{-1}$ – $D_{\text{NO-H}}$ relationship. For the system involving HA **14a**, **15a**, **15b**, **15c**, or **16a** and NR **10**, this relationship is described by the equation

$$\log k_{-1} = 21.06 - 0.24D_{\text{NO-H}} \quad (2)$$

The $D_{\text{NO-H}}$ values for HAs **14a**, **15a**, **15b**, and **15c** were determined in the present work, and $D_{\text{NO-H}}$ for HA **16a** is reported in [13]. The rate constants k_{-1} of the corresponding reactions were either determined in this study (Table 1) or taken from [23]. Knowing k_{-1} for the HA **13a**–, **17**–, and **20**–NR **10** systems (Table 1), we estimated $D_{\text{NO-H}}$ for HAs **13a**, **17**, and **20** using Eq. (2). Furthermore, $D_{\text{NO-H}}$ for HA **13a** was determined using the relationship

$$\log k_{-1} = 17.2 - 0.18D_{\text{NO-H}}, \quad (3)$$

which was established for the HA **14a**–, **15b**–, and **15c**–NR **22** systems. The $D_{\text{NO-H}}$ values calculated for HA **13a** by Eqs. (2) and (3) are equal (69.7 and 69.6 kcal/mol). They coincide with the earlier reported experimental value of 69.6 kcal/mol [24] and are close to the calculated value of 70.9 kcal/mol [16, 17]. The $D_{\text{NO-H}}$ value for HA **17** is 69.5 kcal/mol and is close to

the calculated value of 70.6 kcal/mol [17]. The $D_{\text{NO-H}}$ value for HA **20** determined from Eq. (2) was also estimated using the following three relationships:

$$\log k_1 = 10.3 - 0.1D_{\text{NO-H}}, \quad (4)$$

which was established for the reactions of HAs **1**, **2**, and **3** with NR **9**;

$$\log k_1 = 10.96 - 0.1D_{\text{NO-H}}, \quad (5)$$

which was established for the reactions of HAs **1** and **3** with NR **8**; and

$$\log k_1 = 18.8 - 0.22D_{\text{NO-H}}, \quad (6)$$

which was established for the reactions of HAs **1** and **3** with NR **6**. The average of the four $D_{\text{NO-H}}$ values for HA **20** (71.9, 70.6, 70.7, and 69.0 kcal/mol) is 70.6 (± 0.8) kcal/mol.

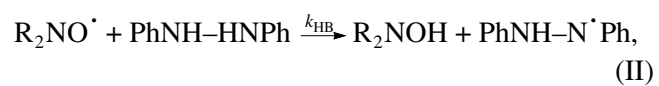
The $D_{\text{NO-H}}$ values obtained for HAs in the present work are given in Table 2.

Using the results of this work and earlier data [23], we related the rate constants of the addition of the hydrogen atom of HA **1** to the five- and six-membered NRs **4**, **5**, **6**, **7**, **8**, **9**, and **21** (k_1) to the $D_{\text{NO-H}}$ values for the corresponding HAs resulting from reaction (I)—**16a**, **17**, **14a**, **15a**, **15b**, **15c**, and **13a**:

$$\log k_1 = -11.48 + 0.23D_{\text{NO-H}}. \quad (7)$$

This relationship demonstrates that the reactivity of a nitroxyl radical is determined by the NO–H bond dissociation energy in the corresponding HA: the stronger the NO–H bond in the HA, the more reactive the NR.

A linear $\log k_{\text{HA}} - \log k_{\text{HB}}$ dependence is reported in [23], where k_{HA} is the rate constant of the reaction between an NR and an HA, and k_{HB} is the rate constant of the reaction between the same NR and hydrazobenzene:



This implies that any reducing agent for which the rate constants of its reactions with these NRs (in particular, with hydrazobenzene as a reducing agent) are known can be used instead of the HA to establish a similar relationship (see Eq. (7)).

Figure 5 plots k_{HB} for the reactions of NRs **4**, **5**, **6**, **7**, **8**, **9**, and **21** with hydrazobenzene (HB) [14] versus $D_{\text{NO-H}}$ for the corresponding HAs **16a**, **17**, **14a**, **15a**, **15b**, **15c**, and **13a** resulting from reaction (II):

$$\log k_{\text{HB}} = -14.53 + 0.22D_{\text{NO-H}}. \quad (8)$$

The $D_{\text{NO-H}}$ values for Eq. (8) were obtained in this study.

Equation (8) and k_{HB} constants for reaction (II) [14, 25] were used to estimate $D_{\text{NO-H}}$ in 80 HAs of the pyrrolidine, pyrrolidinone, imidazoline, and piperidine series.

Table 2. Rate constants of HA formation by reaction (II) (k_{HB}) and dissociation bond energies ($D_{\text{NO-H}}$) in HAs

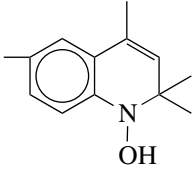
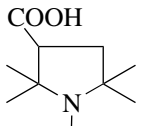
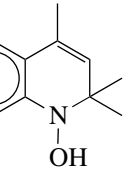
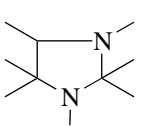
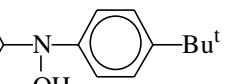
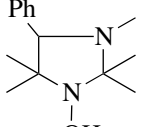
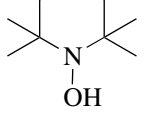
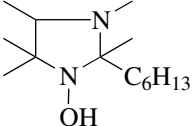
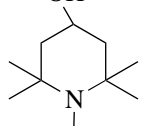
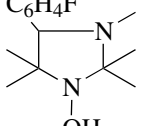
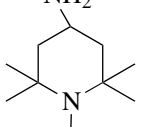
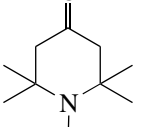
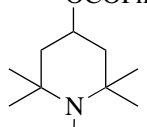
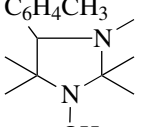
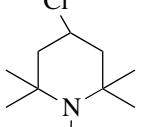
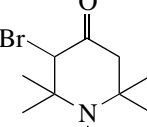
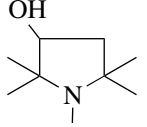
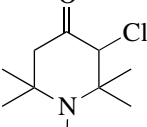
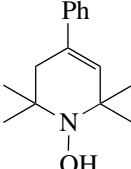
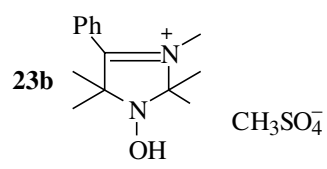
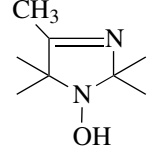
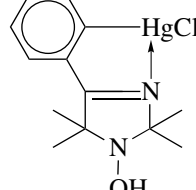
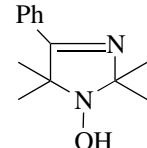
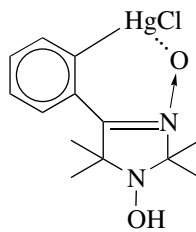
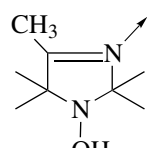
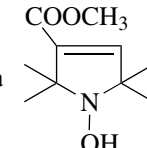
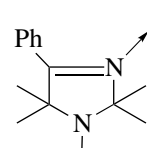
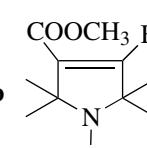
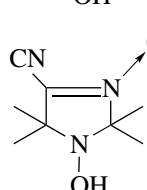
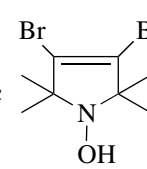
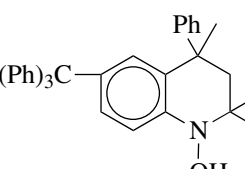
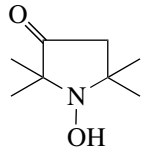
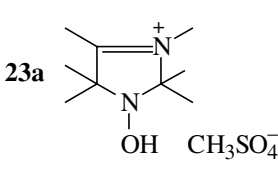
HA	k_{HB} , 1 mol ⁻¹ s ⁻¹	$D_{\text{NO-H}}$, kcal/mol	HA	k_{HB} , 1 mol ⁻¹ s ⁻¹	$D_{\text{NO-H}}$, kcal/mol
1 	—	69.6*	14b 	2.69	68.0
2 	—	65.0*	15a 	1.5	66.5*
3 	—	68.2*	15b 	2.17	66.7*
13a 	8.7	69.7*	15c 	0.37	64.8*
13b 	14.15	71.3	15d 	2.8	68.1
13c 	12.0	70.95	15e 	0.32	67.5
13d 	14.6	71.3	16a 	13.9	71.9 [13]
13e 	13.5	71.2	16b 	27.0	72.6
14a 	1.37	66.4*	16c 	67.0	74.4

Table 2. (Contd.)

HA	k_{HB} , 1 mol ⁻¹ s ⁻¹	$D_{\text{NO-H}}$, kcal/mol	HA	k_{HB} , 1 mol ⁻¹ s ⁻¹	$D_{\text{NO-H}}$, kcal/mol
	6.6	69.5*		209	76.6
	6.8	69.8		11.7	70.9
	4.9	69.2		108	75.3
	43.8	73.5		4.4	69.0
	31.5	72.9		3.6	68.6
	196	76.5		3.2	68.4
	420	70.6		19	71.9
	156	76.0			

* Experimental data.

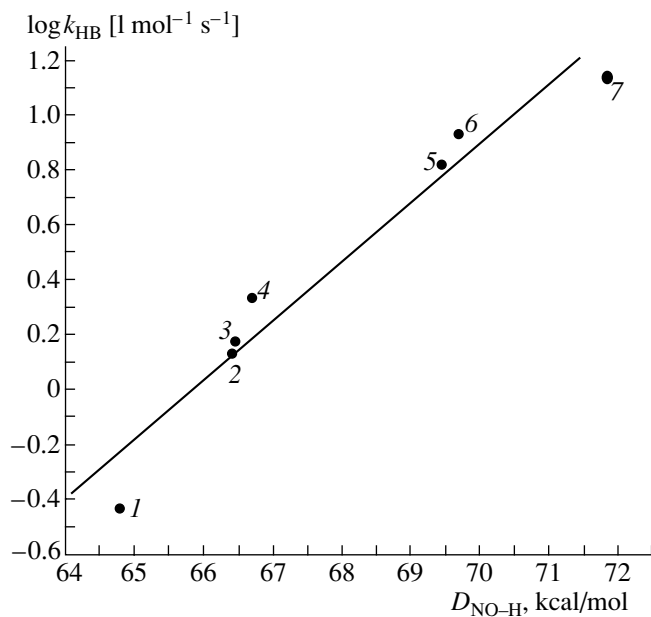


Fig. 5. $\log k_{\text{HB}}$ for the reduction of NRs **4–9** and **21** with hydrazobenzene (HB) versus $D_{\text{NO-H}}$ in the resulting HAs **16a**, **17**, **14a**, **15a**, **15b**, **15c**, and **13a**: (1) NR **9**–HA **15c**, (2) NR **7**–HA **15a**, (3) NR **6**–HA **14a**, (4) NR **8**–HA **15b**, (5) NR **21**–HA **13a**, (6) NR **5**–HA **17**, and (7) NR **4**–HA **16a**.

Some of these bond dissociation energies are presented in Table 2.

The discrepancy between the $D_{\text{NO-H}}$ values calculated using Eq. (8) and the parabolic model of the transition state [16, 17] does not exceed 1–1.5 kcal/mol for any HA.

Note that, if the resulting HA has an intramolecular hydrogen bond or can undergo conformational transitions, as with **13b** (Fig. 1), whose six-membered ring can assume the boat conformation [21] with an intramolecular H bond between the 1-OH and 4-OH groups [13], the NO–H bond dissociation energy calculated for this HA may differ from the observed value. For example, Eq. (8) gives $D_{\text{NO-H}} = 71.3$ kcal/mol, while the experimental value of this energy is reported to be 65.0 kcal/mol [13]. However, this is rarely the case.

The data in Table 2 make it possible to analyze the influence of structural factors (the nature of the ring at a fixed ring size, functional groups in different positions of the ring, etc.) on the dissociation energy of the NO–H bond in HAs.

The presence of a nitrone group in 3-imidazoline HAs increases the bond dissociation energy considerably. Hydroxylamines **18a** and **18b** (without a nitrone group) are characterized by $D_{\text{NO-O}} = 69.8$ and 69.2 kcal/mol, respectively, while the same energy for HAs **19a** and **19b** (with a nitrone group) is 73.5 and 72.9 kcal/mol, respectively. The NO–H bond dissociation energy is especially high if there is a positive charge on the N(3) atom: $D_{\text{NO-H}} = 76.0$ kcal/mol for **23a** and 76.6 kcal/mol for **23b** versus 69.8 kcal/mol for **18a** and 69.2 kcal/mol for **18b**. Furthermore, it increases with increasing electron-withdrawing properties of the functional groups in the positions separated from the NO–H group by two or more σ bonds: $D_{\text{NO-H}} = 73.5$ kcal/mol for **19a** ($R^1 = \text{CH}_3$) and 76.5 kcal/mol for **19c** ($R^1 = \text{CN}$). The bond dissociation energy increases in the order **16a** < **16b** < **16c** ($R^1 = \text{H, Br, Cl}$): $D_{\text{NO-H}} = 71.9$, 72.6, and 74.4 kcal/mol, respectively. The $D_{\text{NO-H}}$ values anticipated for the metal-containing HAs **24** and **25** (70.9 and 75.3 kcal/mol, respectively) are higher than $D_{\text{NO-H}}$ for the similar HAs containing no organometallic functional groups (**18b** and **19b**; $D_{\text{NO-H}} = 69.2$ and 72.9 kcal/mol, respectively). This difference can arise from the induction effects of the intramolecular coordination bonds $\text{N} \longrightarrow \text{Hg}$ and $\text{O} \cdots \text{Hg}$ [25].

REFERENCES

1. Rashba, E., Chernikov, V.A., Baider, L.M., and Vartanyan, L.S., *Biol. Membr.*, 1986, vol. 3, no. 8, p. 838.
2. Toda, T., Mori, E., and Murayama, K., *Bull. Chem. Soc. Jpn.*, 1972, vol. 45, no. 6, p. 1904.
3. Dikanov, S.A., Grigor'ev, I.A., Volodarskii, L.B., and Tsvetkov, Yu.D., *Zh. Fiz. Khim.*, 1982, vol. 56, no. 11, p. 2762.
4. Kartasheva, Z.S., Kasaikina, O.T., Koroteev, S.V., and Malievskii, A.D., *Kinet. Katal.*, 1991, vol. 32, no. 5, p. 1092.
5. Zhdanov, R.I. and Rozantsev, E.G., *Khim.-Farm. Zh.*, 1988, no. 2, p. 147.
6. Komarov, P.G., Toskaeva, O.N., and Zhdanov, R.I., *Dokl. Akad. Nauk SSSR*, 1987, vol. 297, p. 734.
7. Schwartz, M.A., Pazce, J.M., and McConnell, H.M., *J. Am. Chem. Soc.*, 1979, vol. 101, p. 3592.
8. Zhdanov, R.I., Kadenatsi, I.B., and Moshkovskiy, Yu.Sh., *Life Sci.*, 1979, vol. 25, no. 26, p. 2163.
9. Rauchman, E.J., Rosen, G.M., and Kitchell, B.B., *Mol. Pharmacol.*, 1979, vol. 15, p. 131.
10. Kartashova, Z.S., *Cand. Sci. (Chem.) Dissertation*, Moscow: Inst. of Chemical Physics, 1989.
11. Jenkins, T.C., Parkins, M.J., and Siew, N.P.Y., *J. Chem. Commun.*, 1975, no. 2, p. 880.
12. Volodarskii, L.B., Grigor'ev, I.A., Dikanov, S.A., Reznikov, V.A., and Shchukin, G.I., *Imidazolinovye nitrosil'nye radikalы* (Imidazoline Nitroxyl Radicals), Novosibirsk: Nauka, 1988.
13. Buchachenko, A.L. and Vasserman, A.M., *Stabil'nye radikalы* (Stable Free Radicals), Moscow: Khimiya, 1973.
14. Malievskii, A.D., Koroteev, S.V., Shapiro, A.B., and Volodarskii, L.B., *Izv. Akad. Nauk SSSR, Ser. Khim.*, 1990, p. 2575.
15. Denisov, E.T., *Zh. Fiz. Khim.*, 1993, vol. 67, no. 12, p. 2416.
16. Denisov, E.T., *Kinet. Katal.*, 1995, vol. 36, no. 3, p. 387.

17. Denisov, E.T. and Denisova, T.G., *Handbook of Antioxidants Bond Dissociation Energies, Rate Constants, Activation Energies and Enthalpies of Reactions*, 2000.
18. Shikhaliev, Kh.S., Shapiro, A.B., Suskina, V.I., Shmyreva, Zh.V., and Zolukaev, L.P., *Izv. Akad. Nauk SSSR, Ser. Khim.*, 1988, no. 12, p. 2870.
19. Komarov, K.V., Chkannikov, N.D., Suskina, V.I., Shapiro, A.B., Kolomiets, A.F., and Fokin, A.V., *Izv. Akad. Nauk SSSR, Ser. Khim.*, 1989, no. 2, p. 472.
20. Ivanov, Yu.A., Kokorin, A.I., Shapiro, A.B., and Rozantsev, E.G., *Izv. Akad. Nauk SSSR, Ser. Khim.*, 1976, no. 10, p. 2217.
21. Rozantsev, E.G., *Svobodnye iminoksil'nye radikaly* (Free Iminoxy Radical), Moscow: Nauka, 1970.
22. Malievskii, A.D., Koroteev, S.V., Gorbunova, N.V., and Brin, E.F., *Kinet. Katal.*, 1997, vol. 38, no. 4, p. 529.
23. Malievskii, A.D. and Koroteev, S.V., *Izv. Akad. Nauk, Ser. Khim.*, 1998, no. 7, p. 1324.
24. Mahoney, L.R., Mendenhall, G.D., and Ingold, K.U., *J. Am. Chem. Soc.*, 1973, vol. 95, no. 26, p. 8610.
25. Malievskii, A.D., Koroteev, S.V., and Shapiro, A.B., *Izv. Akad. Nauk, Ser. Khim.*, 1993, no. 1, p. 224.